Pergamon

PII: S0306-4522(99)00385-1

www.elsevier.com/locate/neuroscience

Neuroscience Vol. 95, No. 1, pp. 51–62, 2000

0306-4522/00 $20.00+0.00

FUNCTIONAL NEOCORTICAL MICROCIRCUITRY DEMONSTRATED WITH INTRINSIC SIGNAL OPTICAL IMAGING *IN VITRO*

A. KOHN,*† C. METZ,‡ M. QUIBRERA,§ M. A. TOMMERDAHL‖ and B. L. WHITSEL‡‖

*Curriculum in Neurobiology and Departments of ‡Cell and Molecular Physiology, §Statistics and ‖Biomedical Engineering, University of North Carolina at Chapel Hill, Chapel Hill, NC 27599-7545, U.S.A.

Abstract—Intrinsic signal optical imaging was used to record the changes in light transmittance evoked by electrical stimulation in slices prepared from sensorimotor cortex of young adult rats. The spatial characteristics of the optical signal evoked by stimulation of layer II/III, IV, V, or VI were clearly different. Layer IV and V stimulation elicited a radially-oriented region of increased light transmittance which was "hourglass" shaped: its tangential extent was greatest in layers II/III and layer V, and least in layer IV. Layer VI stimulation also elicited a radially-oriented signal but the tangential extent of this signal was the same across layers II–VI—that is, it was column-shaped. Upper layer stimulation produced a signal whose tangential extent was much greater in the upper layers than its radial extent to the deeper layers. The spatial form of the stimulus-evoked intrinsic signal was not dependent on the cytoarchitectonic area in which it was elicited. The tangential and radial distribution of the signal evoked by stimulation of different layers appears to reflect the connectivity of cortex, particularly the horizontal connectivity present in layers II/III, V, and VI, and the interlaminar connections that exist between layers II/III and V and from layers VI to IV. The spatial characteristics of the intrinsic signal were independent of the strength of stimulation used. The idea that inhibitory mechanisms restrict the tangential extent of the signal was evaluated in experiments in which the intrinsic signal was recorded before and after the addition of 10 μM bicuculline methiodide. In all slices studied in this way ($n = 12$), bicuculline methiodide drastically increased the tangential extent of the signal. In 4/12 slices, the tangential spread of the signal was asymmetric with respect to the stimulus site. Asymmetric spread of the signal occurred for both layer V and layer VI stimulation and, in 2/4 of those cases, could be attributed to a cytoarchitectonic border whose presence appeared to restrict the spread of the signal across the border. Although increasing stimulation strength did not change the spatial characteristics of the radially-oriented signal evoked by layer V or VI stimulation, at maximal stimulus intensity the signal evoked from these layers was often accompanied by a band of decreased light transmittance in the most superficial layers (layers I and II).

It is concluded that *in vitro* intrinsic optical signal imaging allows one to image a response attributable to activation of local subsets of cortical connections. In addition, the opposite effects of high-intensity deep layer stimulation on the superficial layers vs layers III–VI of the same column raise the possibility that the most superficial layers may respond differently to repetitive input drive than the rest of the cortical column. © 1999 IBRO. Published by Elsevier Science Ltd.

Key words: optical imaging, intrinsic signal, functional microcircuitry, somatosensory cortex.

The intrinsic optical signal (IOS) is an activity-dependent change in the light scattering properties of neural tissue. The IOS elicited in brain slices by electrical stimulation is thought to reflect changes in the extracellular space following changes in extracellular ion concentrations.[16,20] Specifically, it is thought that repetitive activity in a neuronal population leads to an accumulation of potassium in the extracellular space which is buffered, at least in part, by the surrounding glia. The movement of potassium from the extracellular space into glial cells, by ion pumps, transporters and channels,[21] is accompanied by the uptake of water, leading to cellular swelling. The resultant decrease in the extracellular space causes a change in the refractive properties of the tissue such that the tissue becomes more transparent. The glial cell swelling model for the IOS is based on the following observations: (i) both furosemide and 0 mM extracellular Cl^- solution block the IOS, presumably by affecting a Na^+–K^+–$2Cl^-$ transporter in astrocytes;[16,20] (ii) the time-course (rise and fall time) of changes in the extracellular space is similar to the time-course of the IOS;[16] and (iii) activity-dependent changes in the extracellular space of the rat optic nerve only occur after the differentiation of astrocytes.[24] In addition, it has been established that the IOS recorded *in vitro* depends on synaptic activity: both the removal of calcium ions from the solution in which the slice is bathed and the addition of glutamate receptor antagonists strongly attenuate the signal.[11,19,20] Since the IOS provides information about postsynaptic neuronal activity, it may prove to be a useful tool for investigating the spatial distribution of activity attributable to the different components of intrinsic cortical connectivity.

While a number of studies have addressed the cellular mechanisms which may underlie the IOS *in vitro*, little work has been reported concerning the spatial characteristics of the signal. To date, IOS imaging *in vitro* has been used only to study the properties of neocortical response to repetitive afferent drive delivered at the layer VI/white matter (WM) border.[11,15,16,19] As a result, the spatial specificity of the signal has not been clearly established. Here we report that evaluation of the IOS elicited by applying electrical stimuli to different layers of rat sensorimotor cortex slices provides information about the spatial characteristics of the activity evoked by both inter- and intralaminar cortical connections, and about the functional expression of connections within and between different cytoarchitectonic areas. The results suggest that the IOS has substantial spatial specificity and allows experimental evaluation of the neural mechanisms that mediate the response of cortex to repetitive afferent drive.

†To whom correspondence should be addressed. Tel.: +1-919-966-1291; fax: +1-919-966-6927.

E-mail address: adamk@med.unc.edu (A. Kohn)

Abbreviations: ACSF, artificial cerebrospinal fluid; BMI, bicuculline methiodide; IOS, intrinsic optical signal; RF, receptive field; WM, white matter; VSD, voltage-sensitive dye.

EXPERIMENTAL PROCEDURES

Coronal slices (500 μm; 50 slices from 22 animals) were prepared from the sensorimotor cortex of young adult rats (100–125 g; Sprague–Dawley; Charles River). Following decapitation, the brain was rapidly removed and placed in ice-cold artificial cerebrospinal fluid (ACSF) having the following composition (in mM): NaCl, 118; KCl, 4.8; $CaCl_2$, 2.5; $NaHCO_3$, 25; $MgSO_4$, 1.2; KH_2PO_4, 1.2; and glucose, 10. Slices were cut in ice-cold ACSF using an oscillating tissue slicer (OTS-4000, Electron Microscopy Sciences). Slices were stored in a bath of warmed (30°C), oxygenated (95% O_2, 5% CO_2) ACSF for a recovery period of at least 1 h prior to placement in a recording chamber mounted on an inverted microscope (Diaphot 200, Nikon). Slices were submerged in the chamber, held in place with a fine mesh, and perfused with warmed (28–30°C) oxygenated ACSF at a rate of 1.5–2 ml/min. The composition of the ACSF used in the recording chamber was the same as that in the recovery chamber. For those experiments using bicuculline methiodide or picrotoxin (Sigma), the drug was dissolved in the standard ACSF (warmed and oxygenated) and added to the bath.

A bipolar stimulating electrode (50 μm) was placed in layer II, III, IV, V, VI or at the layer VI/WM border using visible morphological features (pial surface and the layer VI/WM border). Following the experiment, the stimulation location was confirmed on the basis of cytoarchitectonic criteria in Nissl-stained sections (prepared with a cryostat, stained using Cresyl Echt Violett, mounted on glass slides and coverslipped) using the brain atlas of Swanson.[26] The site of stimulus application was, most frequently, in primary somatosensory cortex (the upper and lower limb and trunk representations as well as the barrel field), but in several slices sites in posterior association area (parietal cortex) were stimulated.

Stimuli were 0.2 ms square-wave pulses delivered by a constant-current stimulus-isolation unit attached to a programmable pulse generator (Master 8, AMPI). The viability and functional stability of the slice was monitored using evoked potential recordings. Glass micropipettes filled with 1 M NaCl (impedance 1–2 MΩ) were placed approximately 400 μm from the pial surface (layer III) when layer V or VI stimulation was used, and in layer V when the upper layers were stimulated. Evoked potentials were band-pass filtered (30–300 Hz) and sampled at 20 KHz. A threshold stimulus, defined as the minimum current necessary to generate an evoked potential, was determined for each slice; for the data reported in this paper the threshold current ranged from 30 to 50 μA. Stimulus intensities of 1.0–3.0× threshold, delivered in 3-s trains at a rate of 10 Hz, elicited a strong intrinsic signal that could be generated repeatedly over a time-period of several hours. Stimulus trains were delivered at intervals of 5 min.

Slices were transilluminated using white light from a controlled light source and viewed from below with low-power magnification (×2 or × 4). Images were obtained using a cooled slow-scan CCD camera (Photometrics) mounted on the side port of the microscope. In most experiments, a reference image was taken 800 ms before stimulation began and an additional 19 images were recorded at intervals of 1.3–1.6 s. Thus, the first two images were obtained during stimulus delivery; the subsequent 17 images were recorded after stimulation had ended. In several experiments, images were obtained every 600 ms using a CCD camera with frame transfer capability. The images were identical to those obtained at slower rates and the two data sets were pooled. Difference images were made by subtracting the reference image from each subsequent image. Image intensity was calculated on a pixel-by-pixel basis using the formula $T_{i,SUM} - T_{i,REF}/T_{i,REF}$. Each image presented in this paper is the sum of all 19 difference images. Images were contrast enhanced using a standard histogram equalization procedure. Increases in light transmittance are shown in black, decreases in white.

All experiments were performed in accordance with National Institutes of Health guidelines and with protocols approved by the University of North Carolina Animal Care Committee. Effort was made to minimize animal use and suffering.

RESULTS

Temporal characteristics of the intrinsic optical signal

The time-course of the IOS *in vitro* is quite slow, reaching peak intensity after the end of stimulation and lasting for tens of seconds. We were interested in whether the different spatial components of the IOS developed with distinct time-courses. Figure 1A shows the time-course of an "hourglass" IOS elicited by stimulation delivered at the layer V/VI border (see below) at a temporal resolution of ~600 ms. The signal first appears, albeit weakly, 200 ms (second frame) after the start of the stimulus train. The signal recorded after 800 ms of stimulation (third frame) has the same spatial form observed in all subsequent frames. Thus, although the temporal resolution of our imaging system is limited, it appears that the intrinsic signal at all locations within an hourglass-shaped territory located immediately above the stimulus site develops with the same time-course.

Although an IOS can be elicited by a quite brief train of repetitive stimulation (for example, only eight stimuli had been delivered at a rate of 10 Hz before the image in Frame 3 of Fig. 1A was recorded), longer duration stimulus trains elicited a signal with higher signal-to-noise ratio. This becomes evident upon comparison of the IOS in Frame 4 with the IOS in Frames 1–3 of Fig. 1A. As a result, a stimulus paradigm using 10 Hz trains delivered for 3 s was chosen for all subsequent trials. The time-course of the IOS intensity elicited by several different stimulus paradigms is shown in Fig. 1C. Although IOS intensity clearly increases with the number of stimuli applied, the spatial form of the signal elicited with the different conditions remained the same (Fig. 2).

Spatial characteristics of the intrinsic optical signal: layer IV–VI stimulation

Trains of stimuli delivered to layer VI of rat sensorimotor cortex elicited an IOS with distinctly different spatial properties from the IOS elicited by stimulation of layer V. Stimuli delivered to layer VI or at the layer VI/WM border elicited a column-shaped IOS extending continuously from above the stimulating electrode to just below the pial surface (Figs 2, 3; $n = 15$ slices). With this stimulus placement, the tangential extent of the IOS was the same in all cortical layers in which it was present (layers II–VI). Moreover, increasing the stimulus strength—the amount of current delivered to layer VI—resulted primarily in an increase in the strength of the column-shaped signal with little or no effect on its tangential extent (Fig. 3B, C).

In contrast, stimuli delivered to layer V ($n = 12$ slices) consistently elicited an IOS comprised of two major horizontal bands, one in the upper layers (layers II/III) and the other in layer V (an "hourglass" spatial pattern; Fig. 4A, see also Figs 1, 5C). These two bands were separated by a more tangentially limited and often weaker signal in layer IV. In some cases, the signal in layer IV was virtually absent following layer V stimulation (Fig. 5C). As with the IOS elicited from layer VI, changes in the strength of stimuli delivered in layer V resulted primarily in an increase in the strength of the signal at the same loci that exhibited a signal at lower stimulus intensities, thus increasing stimulus strength had little or no effect on the tangential extent of the IOS. Stimuli delivered to layer IV ($n = 5$ slices) resulted in a spatial pattern similar to that observed following layer V stimulation (Fig. 4B): a tangentially restricted signal was evoked in layer IV and a horizontally more extensive signal was evoked in layers II/III and V.

Interestingly, for both layer V and layer VI stimulation, a strong stimulus intensity (>2× threshold) often elicited an

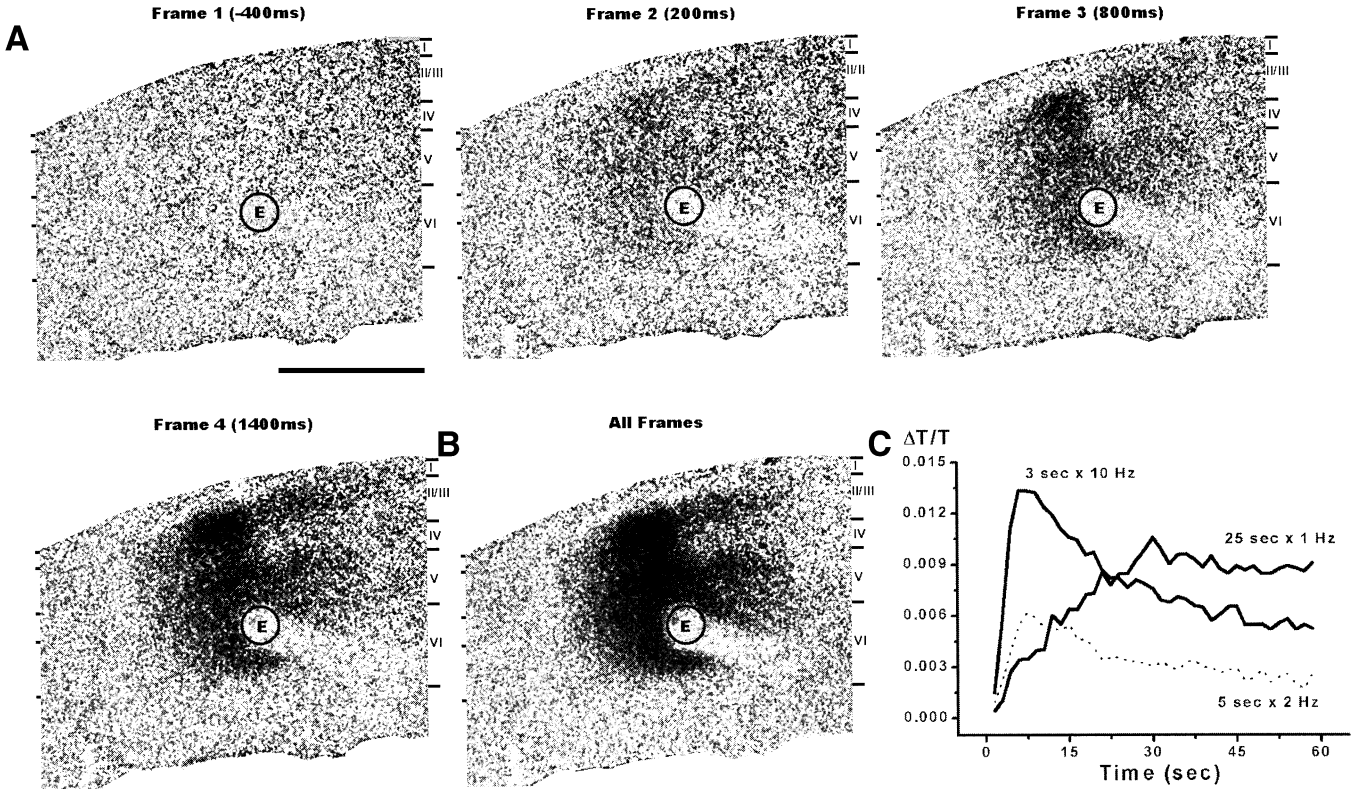

Fig. 1. Time-course of the intrinsic optical signal. (A) Four consecutive frames showing the time-course of the intrinsic optical signal elicited by a train of stimuli (3 s × 10 Hz) delivered to layer V. Frame 1 was obtained 400 ms before stimulation began. Subsequent frames were taken at times indicated. (B) Intrinsic optical signal generated from all frames ($n = 18$) obtained after stimulus onset. (C) Time-course of a 30 × 30 pixel region (containing the peak image intensity) in images evoked by three different stimulus paradigms in a single slice. For this data set only, 40 frames were collected at intervals of 1.5 s. In this and all subsequent figures scale bars for all images are 1 mm, stimulating electrode position is indicated by the letter "E", and image orientation is with the pial surface of the slice to the top.

IOS in the most superficial layers which was opposite in sign to the signal in the region immediately below it (see Figs 5A and 7A). Thus, with both high intensity layer V and layer VI stimulation, layers I and II often showed a decrease in light transmittance at higher stimulus intensities, while layers III–VI in the same column showed an increase in transmittance.

Spatial characteristics of the intrinsic optical signal: upper layer stimulation

Unlike stimulation delivered to layer V or VI, stimulation at sites in the upper layers (50–300 μm below the pial surface, $n = 14$ slices) elicited IOSs that were not radially oriented. Rather, the signal elicited by upper layer stimulation consisted of a tangentially extensive band of activity in the upper layers which decreased progressively in intensity as the deep layers were approached (Fig. 4C; $n = 11$ slices). In one slice, the band in the upper layers was paralleled by a second similarly oriented band in the lower layers (Fig. 4D, E). Between these two IOS bands was a region of weaker signal in layer IV. Stimuli delivered deeper in the upper layers (400 μm below the surface) resulted in an IOS consisting of one tangential band of activity extending across the upper layers with a narrower radial band of signal extending as a column to the lower layers (IV–V) (Fig. 4F; $n = 6$ slices). As was the case with lower layer stimulation, an increase in the intensity of stimuli delivered to the upper layers resulted in an increased magnitude of the signal, but had little or no effect on its tangential extent (Fig. 4D, E). No regions of decreased light transmittance were observed following upper layer stimulation, even when quite strong stimulus intensities (3 × threshold) were used.

Effects of inhibitory block

The observation that the IOS evoked by layer V or VI stimulation remained unchanged in its tangential extent, even with substantial increases in stimulus intensity, led us to test the possibility that stimulus-evoked inhibitory mechanisms were constraining the tangential spread of the signal. The results obtained following a brief application of 10 μM bicuculline methiodide (BMI) to the slice were fully consistent with this idea: BMI caused a dramatic increase in both the intensity and tangential extent of the IOS ($n = 11$ slices, Fig. 5). In addition, the manner in which the tangential extent of the IOS was modified after exposure to BMI depended on the initial (predrug) spatial pattern type. More specifically, application of 10 μM BMI to a slice in which trains of stimuli to layer VI elicited a column-shaped IOS caused a tangential spread of the IOS that was the same in the upper layers (II/III), the deep layers (V/VI) and in layer IV (Fig. 5A, B). As a result, the columnar shape of the response was maintained after exposure to BMI, although at the peak of the drug effect the column-shaped signal was substantially wider in tangential dimension than it was prior to BMI treatment. Similarly, in slices in which an hourglass-shaped signal was elicited by a train of stimuli delivered to layer V, BMI application caused a dramatic increase in the tangential extent of the IOS in both

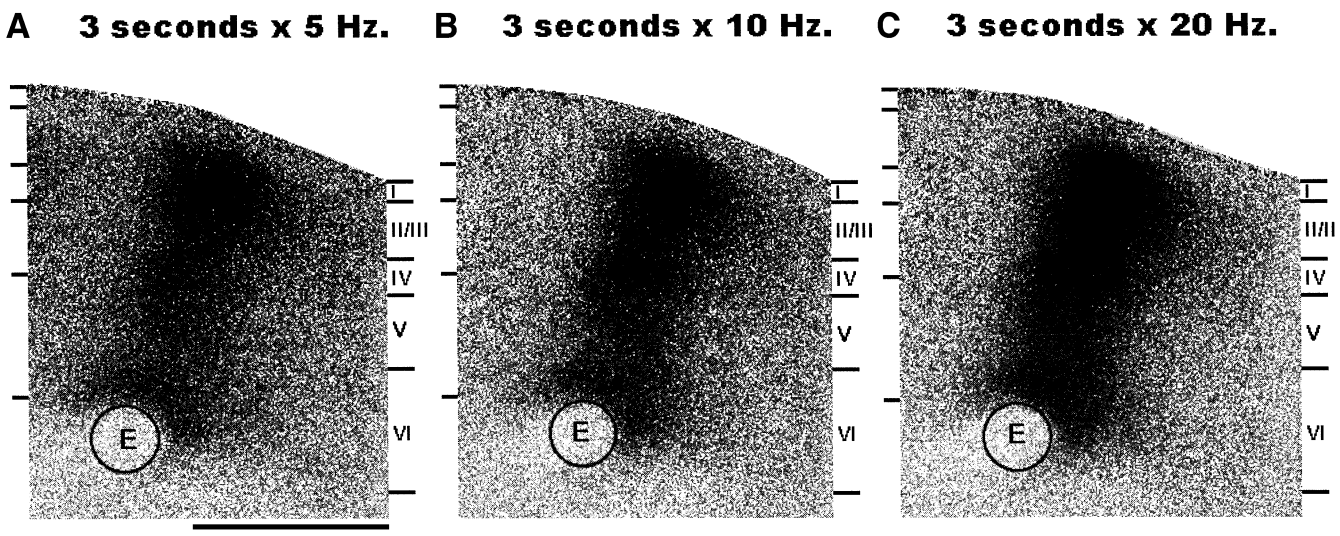

Fig. 2. The effect of changes in the frequency of stimulation on the spatial characteristics of the intrinsic optical signal. Column-shaped patterns following layer VI/white matter stimulation were observed with three second trains of stimuli delivered at 5 Hz (A), 10 Hz (B), and 20 Hz (C).

the upper layers (II/III) and layer V, but relatively little or no change in layer IV (Fig. 5C, D). In four out of 11 slices treated with 10 μM BMI, the increase in tangential extent of either the hourglass or column-shaped signals after drug treatment increased asymmetrically about the stimulating electrode (described in more detail below). Finally, in those cases in which the predrug IOS included a band of decreased light transmittance in layers I/II, 10 μM BMI consistently eliminated this component of the signal (four out of four slices; Figs 5A, 7A, B). Recovery from the BMI-mediated block of $GABA_A$ conductances consisted both of a reversion of the stimulus-evoked IOS to its original spatial extent and a reappearance of the band of decreased light transmittance observed in the most superficial layers.

Recently, BMI has been shown to block the small conductance Ca^{2+}-activated potassium channel responsible for slow afterhyperpolarization.[8] Consequently, the results obtained with BMI could be due to a direct excitatory effect rather than to disinhibition mediated by $GABA_A$ receptor block. To test this possibility, we recorded the IOS in three slices before and after a brief exposure to 100 μM picrotoxin ($n = 3$ slices). Picrotoxin treatment had an effect similar to BMI, resulting in a dramatic increase in the tangential extent of the IOS elicited from layer VI (not shown).

Effect of cytoarchitectonic areas and borders

To evaluate the possibility that the spatial properties of the IOS were determined by morphological variables such as the cortical area in which the stimuli were delivered and not by the laminar site of stimulation, Nissl-stained sections were prepared from the slices from which functional images had been obtained. No relationship was found between the cytoarchitectonic area in which the stimuli had been applied and the spatial pattern type observed. For example, layer VI stimulation in both barrel field and non-barrel field (upper limb representation) sensorimotor cortex elicited a column-shaped activity pattern (Fig. 6). Indeed, for slices taken from a ~ 5 mm anterior-posterior range ($+1.0$ mm bregma to -4.0 mm bregma) and with stimulation sites from a near medial location to 6 mm lateral to the midline, the spatial characteristics of the signals elicited by stimulation in a given layer were remarkably similar. The sites to which stimuli were applied were predominantly in primary somatosensory cortex (the upper and lower limb and trunk representations as well as the barrel field) but for several slices were in posterior association area (parietal cortex).[26]

While the spatial form of the IOS was independent of the cytoarchitectonic or functional area in which it was elicited, the IOS spread under inhibitory block did appear to respect cytoarchitectonic borders. In two cases it was found that the asymmetric spread of activity under BMI treatment coincided with the presence of a cytoarchitectonic border. More specifically, in both of those cases the IOS exhibited a tangential spread within the cytoarchitectonic area which included the stimulation site, with the lateral spread in the other direction ending abruptly at the location of a distinct cytoarchitectual border. Figure 7 shows an example in which the signal extends tangentially for a large distance within the cytoarchitectonic area (non-barrel field cortex) to which the stimulus was applied, but extends only slightly into the adjacent cytoarchitectonically distinct area (barrel field cortex).

DISCUSSION

The observed changes in the spatial characteristics of the IOS that accompany changes in the laminar position of the stimulating electrode, the relative insensitivity of the IOS to changes in stimulation strength, the molding of the IOS by stimulus-evoked inhibitory mechanisms, and, finally, the possible influence of cytoarchitectonic borders on the IOS, all suggest that the signal reflects the functional connectivity of cortex. In addition, the observation that the component of the IOS in layers I and II often includes a decrease in light transmittance, while the component in layers II to VI consists of an increase in transmittance, suggests that the columnar response of cortex to layer VI stimulation may involve different processes in the most superficial and deeper cortical layers.

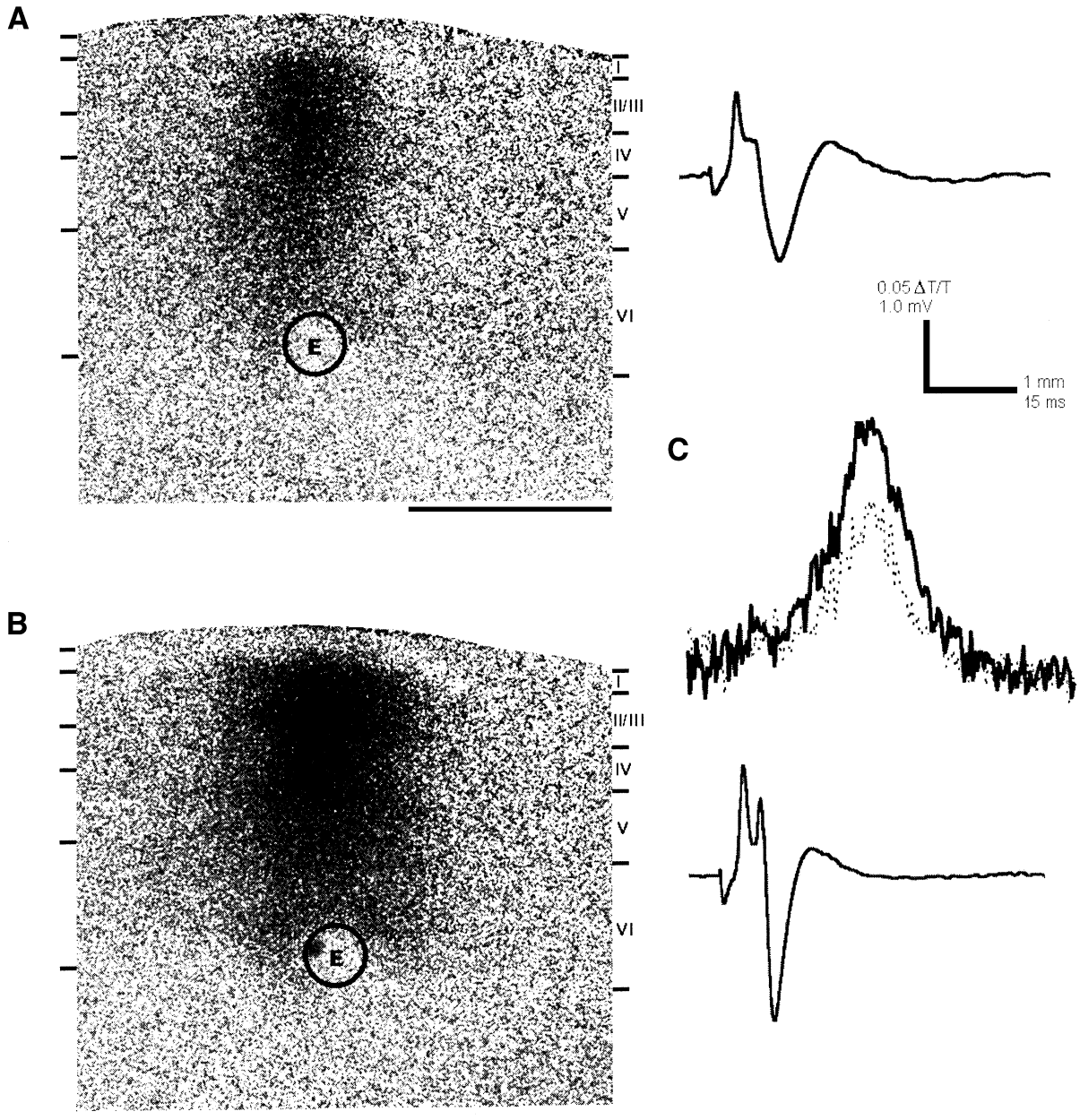

Fig. 3. The effect of changes in stimulus strength on intrinsic optical signal spatial patterns elicited from the layer VI/white matter border. (A) Column-shaped activity pattern elicited by a pulse train delivered in layer VI. Evoked potential elicited by the first stimulus of the train used to elicit the intrinsic optical signal is shown to the right of the image. (B) A doubling of the stimulus intensity (from 1.5 × threshold to 3.0 × threshold; threshold = 50 μA) increases the intensity of the intrinsic optical signal but has little effect on the tangential extent of the signal. Evoked potential elicited by the first stimulus of the train used to elicit the intrinsic optical signal is shown to the right of the image. (C) Tangential intensity distribution for the two images. The distribution for the image in (A) is shown with the broken line. Each point in the intensity distribution represents the average intensity of pixels in a single-pixel wide column extending from the pial surface to the location of the stimulating electrode. Both distributions were smoothed with a moving average filter to facilitate comparison. Scale bar for panels A and B is shown under panel A (1 mm). The scale bar for the evoked potentials and the intensity distribution is shown in the upper right.

Functional imaging of cortical connectivity

The dependence of the spatial characteristics of IOS activity patterns on the laminar position of the stimulating electrode used to elicit them, their insensitivity to changes in the intensity of stimulation, and the effect of blocking $GABA_A$ conductances with BMI, leads to the model of cortical circuitry presented in Fig. 8. The arrows in Fig. 8 indicate the minimum intra- and interlaminar connectivity needed to explain the spatial characteristics of the functional images and does not include all known interlaminar cortical connections. The interlaminar arrows in Fig. 8 indicate the presence of functional connectivity between two layers without implying a direct input from one to the other (due to the difficulty in distinguishing between ortho- and antidromically relayed activity; see below). The IOSs evoked by layer V stimulation, a prominent signal in both layers II/III and V with relatively weak or no signal in layer IV, suggests the existence of a strong functional connectivity between layer V and layers II/III that avoids layer IV. The large tangential extent of the signal in layers II/III and V presumably reflects the presence of a rich horizontal connectivity in those layers.

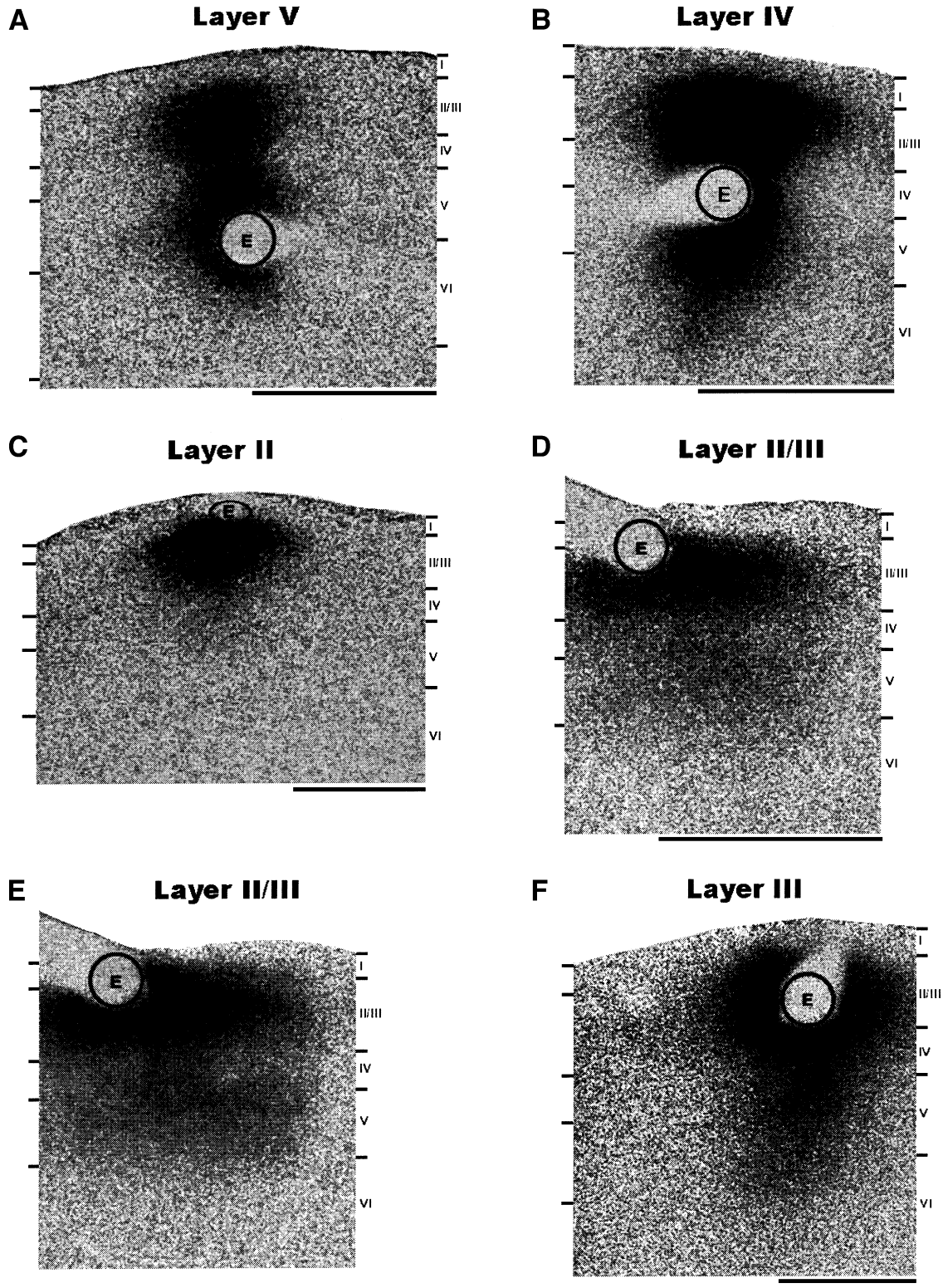

Fig. 4. Intrinsic optical signal elicited by stimuli delivered to different cortical layers. (A) Hourglass-shaped activity pattern elicited by stimulation in layer V. Note the narrow band of activity in layer IV relative to the bands in the upper layers and layer V. (B) Layer IV stimulation elicits an intrinsic optical signal similar to (A). (C) Intrinsic optical signal with an extensive tangential but limited radial extent elicited by stimulation in layer II. (D) Stimulation delivered to layer II/III elicits an intrinsic optical signal with tangentially extensive bands in both the upper layers and layer V, and with a reduced intensity in layer IV. (E) Intrinsic optical signal elicited in the same slice using a higher stimulus strength (100 μA instead of 55 μA). (F) Intrinsic optical signal elicited by layer III stimulation consisting of a tangentially extensive band in the upper layers and a narrower band extending to layer V.

Similarly, the restricted width of the signal in layer IV, observed following both layer V and layer IV stimulation, presumably reflects the absence of horizontal connectivity in layer IV. The variable strength of the signal in layer IV following layer V stimulation could be ascribed to the strength of thalamocortical input recruited by our stimulus

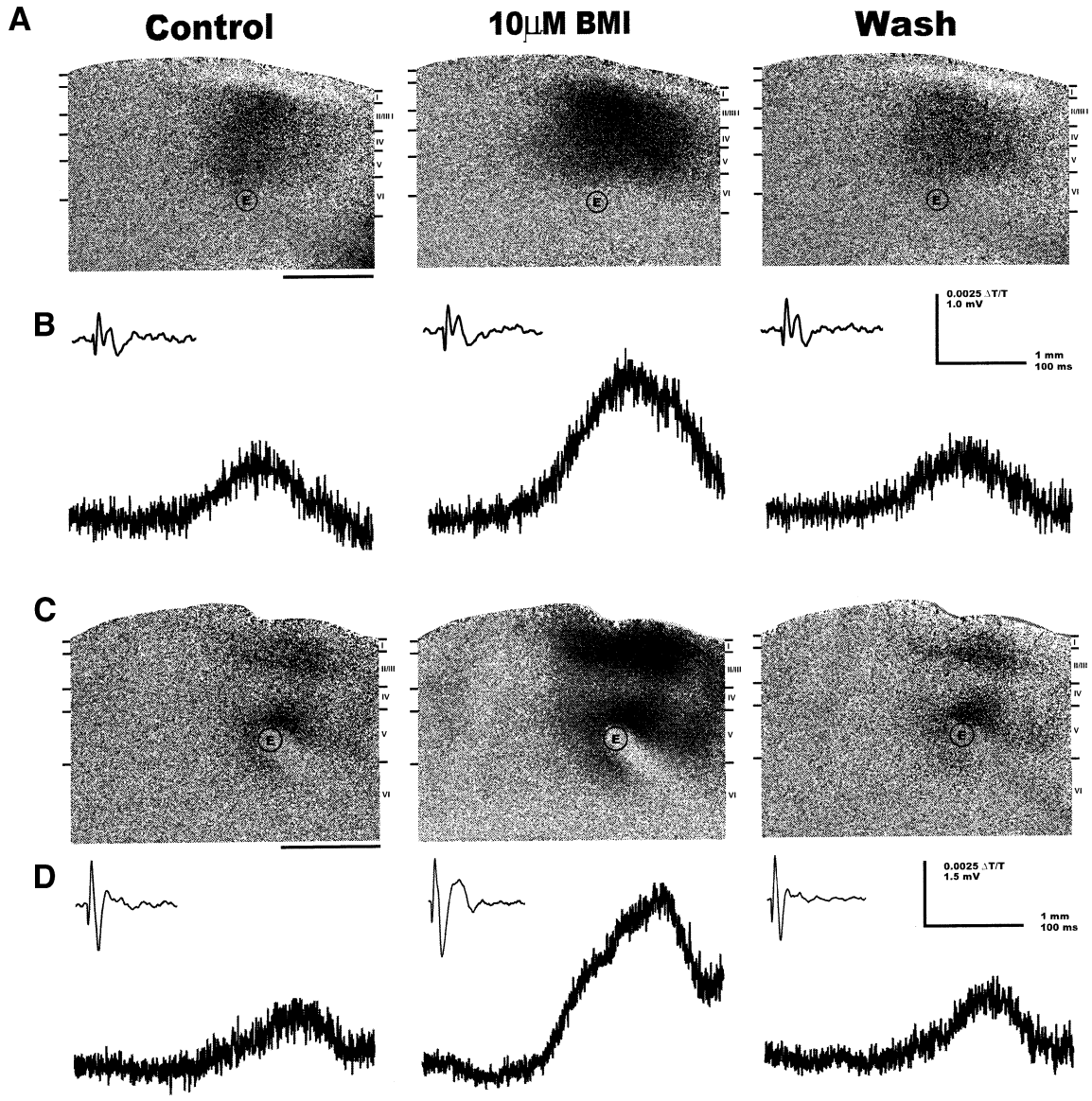

Fig. 5. Effect of BMI on intrinsic optical signal spatial activity patterns. (A) Control, drug effect, and postdrug recovery for a column-shaped activity pattern elicited by a train of stimuli applied to layer VI. Note that a clear band of decreased light transmittance exists just below the pial surface in the control image, and that this part of the signal is blocked by the application of 10 μM BMI. (B) Bottom—tangential intensity distribution for each image shown in (A); Top—evoked potential elicited by the first stimulus in the train. (C, D) Same format as in (A, B) for an "hourglass" activity pattern elicited by a train of stimuli applied to layer V. Note that BMI caused an increase in the tangential extent of the signal in the upper layers and layer V, but did not change either the intensity or tangential extent of the intrinsic optical signal in layer IV. Each point in the intensity distributions represents the average intensity of pixels in a single pixel-wide column extending from the pial surface to the location of the stimulating electrode.

at that cortical location. Layer II/III stimulation resulted in a band of activity in layer V in only one slice out of the 11 tested, suggesting a similar, albeit weaker, functional connectivity from layer II/III to V. However, in all cases of upper layer stimulation, the tangential extent of the IOS in the supragranular layers was greater than in layer IV, indicative of the excitatory horizontal connections deriving from pyramidal cell axon collaterals in layers II/III.

In contrast to layer V stimulation, trains of stimuli delivered in layer VI elicited a column-shaped IOS with equal tangential extent across all layers. Why is it that stimulation in layer VI leads to a signal in layer IV which has the same tangential extent as in layers II/III, V and VI, while layer V stimulation produces a tangentially extensive IOS in layers II/III and V, but only a very narrow band of activity in layer IV? A possible explanation is the presence of horizontal connectivity in layer VI and of excitatory axonal collaterals from layer VI pyramidal cells to layer IV neurons. In this view, the signal in layer IV is generated by two inputs. A narrow IOS signal is generated in layer IV by thalamocortical input (as with layer V stimulation) which is filled-in or widened by a projection from layer VI pyramidal cells. The images obtained under inhibitory conductance block are consistent with this model of cortical connectivity. When there was a tangential spread of the IOS in layer VI, the spread of the IOS in layer IV matched that in layer VI; when there was little or no signal in layer VI, blocking inhibition failed to lead to a tangential spread of activity in layer IV. In addition, the IOS generated during BMI treatment was found to respect cytoarchitectonic borders—at least

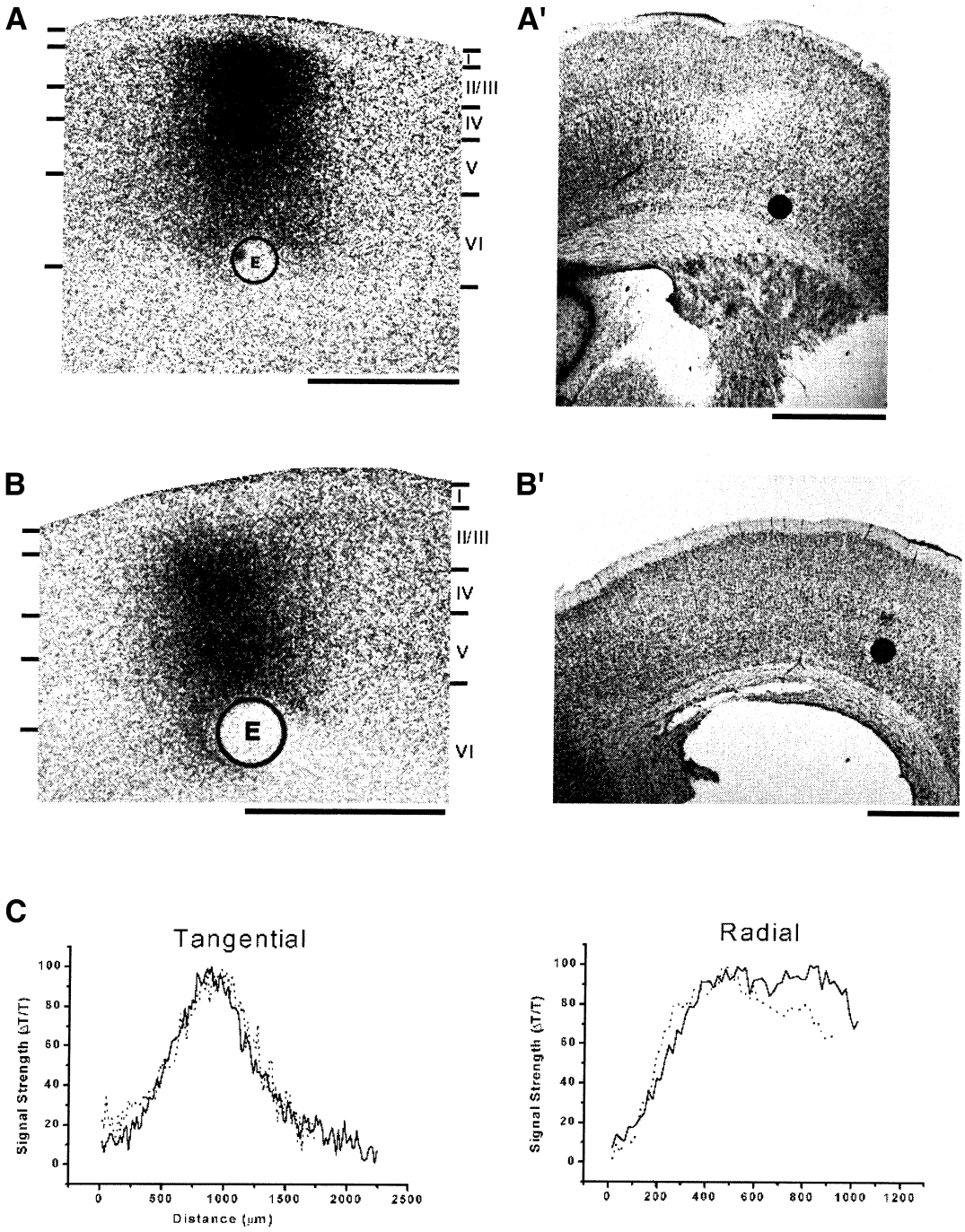

Fig. 6. Comparison of intrinsic optical signal elicited in two different cytoarchitectonic areas. (A, B) Images of column-shaped activity patterns elicited in two different slices by stimulation applied in layer VI. Stimulus parameter for both slices was a train of 30 stimuli (3 s at 10 Hz) at a current strength of 2.0 × threshold. (A′ and B′) Nissl-stained sections obtained from the slices that yielded the images shown in (A) and (B). Black dots in the Nissl sections indicate the position of the stimulating electrode. The slice shown in the top right panel is from ~3.5 mm posterior to bregma; the stimulus location is 3.5 mm lateral from the midline. The slice on the bottom right is from ~1 mm anterior to bregma; the stimulus location is 4 mm lateral from the midline. Section orientation: medial to the left. (C) Scaled tangential and radial segmentation plots showing the intensity distributions for intrinsic optical signals shown in A and B. The distributions obtained by radial and tangential segmentation were smoothed with a moving average filter to facilitate comparison.

those borders which were substantial enough to be detected in the Nissl-stained sections we prepared from each slice.

Electrical stimulation of the type used in this study elicits both antidromic and orthodromic activity. We and others have previously shown that the IOS requires postsynaptic activation since the removal of Ca^{2+} ions from the solution with which the slice is perfused leads to a total but reversible loss of the signal.[19,20] Similarly, the application of the glutamate receptor antagonists D-2-amino-phosphovaleric acid (D-APV, 100 μM) and 6-cyano-7-nitroquinoxaline-2,3-dione (CNQX, 10 μM)[11] or kynurenic acid (1.5 mM)[20] leads to an almost complete block of the IOS. Thus, the IOS does not appear to reflect antidromic activity directly. Of course, antidromically-conducted activity which is relayed synaptically to a postsynaptic cell should contribute to the signal. As a result, the spatial patterns described above reflect functional

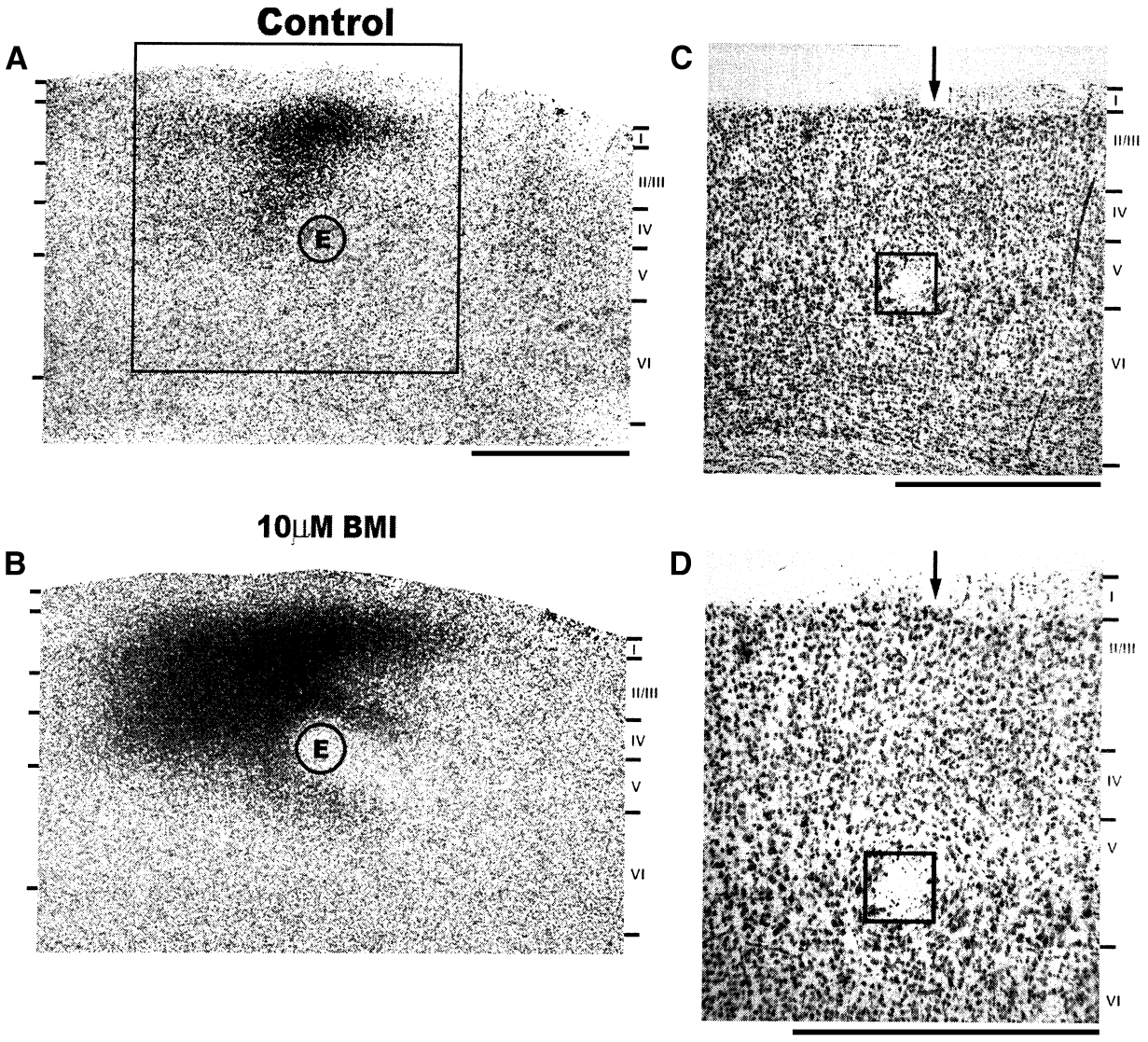

Fig. 7. Effect of BMI on intrinsic optical signal elicited near a cytoarchitectonic border. (A) The initial spatial pattern elicited by an electrode placed at the border of layer VI and layer V. This signal shows tangential spread of activity (presumably mediated by horizontal connections) towards the right of the image and a lesser spread to the left. The black box delineates the region shown in the Nissl-stained section in (C). (B) Effect of 10 μM BMI. (C) Low-magnification (×4) image of a Nissl-stained section obtained from the same slice. Position of the stimulating electrode is enclosed by the black-framed box. Arrow indicates locus of cytoarchitectonic transition between non-barrel (upper limb representation) and barrel field cortex. Section orientation: medial to the left. (D) Higher-power (×6.3) image of the same section.

connections originating in a particular layer as well as axons projecting to that layer. For instance, the IOS generated in layer V following layer VI/WM stimulation reflects both orthrodromically relayed activity (for example, activity relayed to layer V via layer IV) and inputs to layer V generated by the backfiring of pyramidal cell axons leaving cortex from layer V.

Comparison with other anatomical, neurophysiological, and optical imaging studies

This report is the first to use IOS imaging to study the functional microcircuitry of cortex *in vitro*. Other studies using IOS imaging *in vitro* have reported only on the properties of neocortical response to repetitive afferent drive delivered at the layer VI/WM border.[11,15,16,19] As a result, some confusion has arisen as to the spatial specificity of the intrinsic optical signal. However, the similarity of our images of functional cortical connectivity with those obtained using voltage-sensitive dye imaging, as well as our observation that the IOS elicited by layer VI/WM stimulation contains mini-column-scale periodicities,[19] suggests that the IOS has substantial spatial resolution.

The functional connectivity suggested by our results is consistent with the findings reported by anatomical studies. The collaterals of layer II/III and V pyramidal cells have been found to provide long-range horizontal connections in those layers in a number of species and cortical areas including rat somatosensory cortex.[7,22] Interlaminar connections between layers II/III and V have also been described in rat somatosensory cortex.[5] The presence of long-range horizontal connectivity in layer VI similar to that observed in layers II/III and V has been documented in the somatosensory cortex of the rat using a number of different labeling techniques including rhodamine-coated microspheres[22] and biocytin.[30] Projections from layer VI to layer IV are also known to

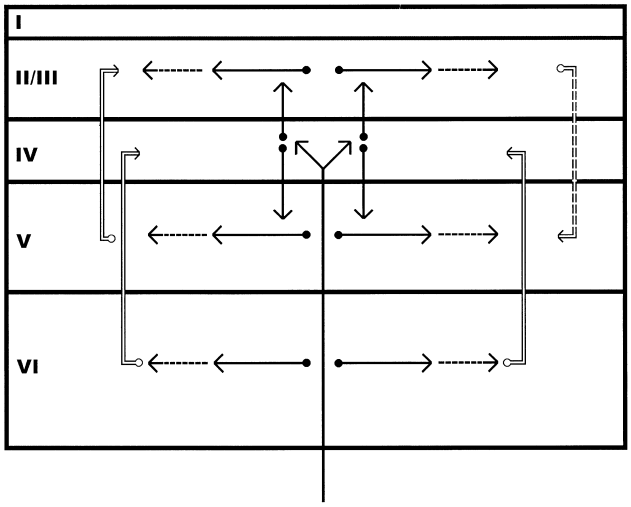

Fig. 8. Minimum features of cortical connectivity needed to explain the functional images obtained with intrinsic signaloptical imaging. Interlaminar connections from layer V to II/III and from layer VI to IV are shown by open arrows. The interrupted open arrow from II/III to V represents the weak interlaminar connectivity observed between these layers. Horizontal connections in layers II/III, V and VI are shown by continuous arrows; interrupted arrows indicate the horizontal connectivity observed when GABAergic inhibition is attenuated by BMI. Arrows originating in layer IV represent the axons of spiny stellate cells which distribute activity radially within the cortical column. Arrows do not indicate the direction of neuroanatomical connectivity since the IOS reflects synaptic activity relayed both antidromically and orthodromically; rather, arrows indicate that it is possible to drive activity in the recipient layer with stimuli delivered at its starting point.

exist, although whether they target predominantly inhibitory or excitatory interneurons has been a subject of debate. Ahmed *et al*. report that layer VI pyramidal cells are the main source of excitatory input to layer IV spiny stellates in the cat visual cortex[1] while White and Keller report that the same projection in the mouse somatosensory cortex is primarily onto inhibitory interneurons.[28] Unfortunately, the method of IOS imaging does not allow one to distinguish between excitatory projections onto inhibitory or excitatory interneurons. Layer IV itself contains little horizontal connectivity.[5]

The presence of horizontal connectivity in the supragranular and infragranular layers is believed to contribute to the large receptive fields (RFs) of neurons in those layers. Similarly, the lack of horizontal connectivity in layer IV is believed to result in the relatively small RFs recorded in that layer. A number of studies have discussed the presence of a functional "hourglass," the waist of which is located in layer IV and indicative of the spatially restricted RFs found there.[6,25] However, other studies have failed to find a difference in RF size in layer IV and have concluded that RF size is independent of the laminar location of the recorded neuron.[18] Interestingly, hourglass-shaped IOS patterns were observed in the present study following layer IV and V stimulation, but not following stimulation delivered at the layer VI/WM border, a location usually chosen for allowing the most physiological stimulation of cortex. The difference between functional hourglass and columnar patterns recorded *in vivo* could be due to differences in anesthetic or stimulus conditions among studies. Our results suggest that the experimental conditions which result in RFs of equal size in all layers may also be particularly favorable for driving cells in layer VI. Such an explanation would rely on the presence of layer VI projections to layer IV to provide input from distal RF locations. Finally, the functional connectivity suggested here is consistent with that proposed by Armstrong-James and colleagues in a study of the laminar dependence of neuronal response latency.[4]

The results of this study, both the model of cortical connectivity and the images underlying it, are similar to those obtained in previous studies using voltage-sensitive dyes (VSDs).[2,3,27,29] There are, however, several important distinctions between this study and the previous VSD studies. First, in VSD studies removal of calcium from the solution that perfused the slices had little effect on the fast-component of the VSD signal, leading the authors to conclude that this component of the signal was largely a result of presynaptic or antidromic activity.[2,3,29] These previous studies also reported components of the VSD which did depend on postsynaptic activity, but this signal was found either to be spatially non-specific,[29] or to occur in a restricted region of the previously active area[2,3] (but see also Refs 12 and 13). In contrast, we and others have shown that the IOS is strongly dependent on postsynaptic activity since removing extracellular calcium ions blocks the IOS almost entirely.[19,20] Thus, although images obtained using VSDs and IOS imaging are quite similar, the IOS is strongly dependent on postsynaptic activity while the VSD signal includes a large component which is not. Second, the present experiments investigated the role of inhibitory mechanisms in sculpting each of the activity patterns while, to our knowledge, similar experiments have not been reported for VSD imaging. Third, the present results suggest that the mechanism responsible for generating the IOS works in opposite ways in the most superficial layers and the rest of the cortical column (see below). Similar observations have not been reported using VSDs. Finally, since the signal discussed here is "intrinsic", it may represent a spatially localized, but temporally delayed, physiological mechanism that alters subsequent neuronal response. If so, the IOS may measure a process important in the response of cortex to repetitive drive (see below).

The intrinsic optical signal and its potential importance

What is the basis of the *in vitro* IOS? Although it is well established that the signal elicited by electrical stimulation requires activation of postsynaptic receptors, the precise mechanism responsible for the generation of the IOS *in vitro* is not entirely clear. It has been proposed by several groups that the signal is a result of astrocytic swelling subsequent to extracellular potassium accumulation.[16,20] Neurons are less susceptible to cell swelling and are thus unlikely to contribute to the IOS.[14] The astrocytic cell swelling model for the IOS is based on the observation that both furosemide and 0 mM Cl^- solution block the IOS, presumably by affecting a Na^+–K^+–$2Cl^-$ transporter in astrocytes;[16,20] that the time-course (rise and fall time) of changes in the extracellular space are similar to the time-course of the IOS;[16] and that activity-dependent changes in the extracellular space of the rat optic nerve only occur after the differentiation of astrocytes.[24]

The results presented here do not significantly contribute to or detract from the above model, although our observation of an opposite light transmittance band in the most superficial layers is not easily explained by it. More recently, however, Holthoff *et al*. have proposed an explanation for the IOS

which could account for the opposite light transmittance changes observed in the most superficial layers.[17] Their model relies on the directed potassium spatial buffering model of Dietzel *et al*. in which potassium accumulation is most substantial in the middle layers and astrocytic buffering of these changes includes uptake of potassium in the middle layers and a parallel release of potassium near the pial surface[9,10] (a form of the spatial buffering hypothesis of Orkand *et al*.[23]). In this model, the release of potassium at the pial surface by astrocytes leads the cells in this local region to shrink, with a resultant increase in the extracellular space and decrease in light transmittance. Although such a model could explain the presence of the opposite light transmittance change observed at higher stimulus intensities, one would expect that the increased neuroelectric activity that occurs under BMI block would lead to greater potassium accumulations in the middle layers, and thus to an increase in the intensity of this band of activity, rather than to its elimination as was observed. Presently, however, we have no alternative explanation for the presence of the band of decreased light transmittance in the upper layers.

Although the basis of the IOS is not entirely understood, we propose that both its spatial and temporal characteristics may make it useful for studies of mechanisms of information processing in neocortex. First, although the signal is spatially specific it is clearly decoupled in time from the neuronal activity which elicits it. Not only does the signal rise slowly and peak after neuroelectric activity has stopped, but the IOS takes tens of seconds to disappear (Fig. 1 and Refs 15, 16 and 20). Thus, the IOS may identify regions of previously active cells. If IOS signal reflects changes in the extracellular space or the concentration of extracellular ions or neuroactive substances, neurons in a region in which an IOS is present may respond differently to further stimulation than they would otherwise. If this proves to be correct, the IOS could be useful for studies of the mechanisms by which repetitive activity induces dynamic changes in the state of cortical neurons and circuits. Experiments designed to test this hypothesis are currently being conducted in our laboratory.

Acknowledgements—We thank Mel Roberts and Olivier Monbureau for technical assistance. This work was supported by a grant from the Whitehall Foundation.

REFERENCES

1. Ahmed B., Anderson J. C., Douglas R. J., Martin K. A. C. and Nelson J. C. (1994) Polyneuronal innervation of spiny stellate neurons in cat visual cortex. *J. comp. Neurol.* **341,** 39–49.
2. Albowitz B. and Kuhnt U. (1993) Evoked changes of membrane potential in guinea pig sensory neocortical slices: an analysis with voltage sensitive dyes and a fast optical recording method. *Expl Brain Res.* **93,** 213–225.
3. Albowitz B. and Kuhnt U. (1993) The contribution of intracortical connections to horizontal spread of activity in the neocortex as revealed by voltage sensitive dyes and a fast optical recording method. *Eur. J. Neurosci.* **5,** 1349–1359.
4. Armstrong-James M., Fox K. and Das-Gupta A. (1992) Flow of excitation within rat barrel cortex on striking a single vibrissa. *J. Neurophysiol.* **68,** 1345–1358.
5. Bernardo K. L., McCasland J. S., Woolsey T. A. and Strominger R. N. (1990) Local intra- and interlaminar connections in barrel cortex. *J. comp. Neurol.* **291,** 231–255.
6. Chapin J. K. (1986) Laminar differences in sizes, shapes, and response profiles of cutaneous receptive fields in the rat SI cortex. *Expl Brain Res.* **62,** 549–559.
7. Chapin J. K., Sadeq M. and Guise J. L. U. (1987) Corticocortical connections within the primary somatosensory cortex of the rat. *J. comp. Neurol.* **263,** 326–346.
8. Debarbieux F., Brunton J. and Charpak S. (1998) Effect of bicuculline on thalamic activity: a direct blockade of I_{AHP} in reticularis neurons. *J. Neurophysiol.* **79,** 2911–2918.
9. Dietzel I., Heinemann U., Hofmeier G. and Lux H. D. (1980) Transient changes in the extracellular space in the sensorimotor cortex of cats in relation to stimulus-induced changes in potassium concentration. *Expl Brain Res.* **40,** 432–439.
10. Dietzel I., Heinemann U. and Lux H. D. (1989) Relations between slow extracellular potential changes, glial potassium buffering, and electrolyte and cellular volume changes during neuronal hyperactivity in cat brain. *Glia* **2,** 25–44.
11. Dodt H. U., D'Arcangelo G., Pestel E. and Zieglgansberger W. (1996) The spread of excitation in neocortical columns visualised with infrared-darkfield videomicroscopy. *NeuroReport* **7,** 1553–1558.
12. Grinvald A., Manker A. and Segal M. (1982) Visualization of the spread of electrical activity in rat hippocampal slices by voltage-sensitive optical probes. *J. Physiol.* **333,** 269–291.
13. Grinvald A., Frostig R. D., Lieke E. and Hildesheim R. (1988) Optical imaging of neuronal activity. *Physiol. Rev.* **68,** 1285–1366.
14. Hertz L. (1981) Features of astrocytic function apparently involved in the response of central nervous tissue to ischemia-hypoxia. *J. Cerebr. Blood Flow Metab.* **1,** 143–153.
15. Holthoff K., Dodt H. U. and Witte O. W. (1994) Changes in rat neocortical slices following afferent stimulation. *Neurosci. Lett.* **180,** 227–230.
16. Holthoff K. and Witte O. W. (1996) Intrinsic optical signals measured with near-infrared dark-field microscopy reveal changes in extracellular space. *J. Neurosci.* **16,** 2740–2749.
17. Holthoff K., Dietzel I. and Witte O. W. (1997) Evidence for a directed spatial potassium buffer mechanism in rat neocortical brain visualised by intrinsic optical signals. *Soc. Neurosci. Abstr.* **23,** 577.17.
18. Ito M. (1985) Processing of vibrissa sensory information within the rat neocortex. *J. Neurophysiol.* **54,** 479–490.
19. Kohn A., Pinheiro A., Tommerdahl M. A. and Whitsel B. L. (1997) Optical imaging *in vitro* provides evidence for the minicolumnar nature of cortical response. *NeuroReport* **8,** 3513–3518.
20. Macvicar B. A. and Hochman D. (1991) Imaging of synaptically evoked intrinsic optical signals in hippocampal slices. *J. Neurosci.* **11,** 1458–1469.
21. Newman E. A. (1995) Glial cell regulation of extracellular potassium. In *Neuroglia* (ed. Knettemann H. and Ransom B. R.), pp. 717–731. Oxford University Press, New York.
22. Nicolelis M. A. L., Chapin J. K. and Lin C.-S. (1991) Ontogeny of corticocortical projections of the rat somatosensory cortex. *Somatosensory Motor Res.* **8,** 193–200.
23. Orkand R. K., Nicholls J. G. and Kuffler S. W. (1966) Effect of nerve impulses on the membrane potential of glial cells in the central nervous system of amphibia. *J. Neurophysiol.* **29,** 788–806.
24. Ransom B. R., Yamate C. L. and Connors B. W. (1985) Activity-dependent shrinkage of extracellular space in the rat optic nerve: a developmental study. *J. Neurosci.* **5,** 532–535.
25. Simons D. J. (1978) Response properties of vibrissa units in rat SI somatosensory cortex. *J. Neurophysiol.* **3,** 798–820.
26. Swanson L. W. (1992) *Brain Maps: Structure of the Rat Brain.* Elsevier, New York.

27. Tanifuji M., Sugiyama T. and Murase K. (1994) Horizontal propagation of excitation in rat visual cortex. *Science* **266,** 1057–1059.
28. White E. L. and Keller A. (1987) Intrinsic circuitry involving the local axon collaterals of corticothalamic projection cells in mouse SmI cortex. *J. comp. Neurol.* **262,** 13–26.
29. Yuste R., Tank D. W. and Kleinfeld D. (1997) Functional study of the rat cortical microcircuitry with voltage-sensitive dye imaging of neocortical slices. *Cerebr. Cortex* **7,** 546–558.
30. Zhang Z.-W. and Deschenes M. (1997) Intracortical axonal projections of lamina VI cells of the primary somatosensory cortex in the rat: a single-cell labeling study. *J. Neurosci.* **17,** 6365–6379.

(*Accepted* 7 *July* 1999)